

# Detection of Weak Random Signals in IID Non-Gaussian Noise

Kevin R. Kolodziejki, *Member, IEEE*, and John W. Betz, *Member, IEEE*

**Abstract**—This paper considers the detection of weak random signals in circularly symmetric, independent, identically distributed noise. Locally optimum detectors and *ad hoc* nonlinearities are considered, with asymptotic expressions provided for evaluation of detection performance. The analytical expressions are used to evaluate the robustness of detectors to mismatch in the noise models. Finite-sample Monte Carlo simulation results indicate the reliability of these asymptotic measures in cases of practical interest. The results show that, as has been found for detection of weak known signals in non-Gaussian noise, reasonably configured *ad hoc* nonlinearities are nearly optimum and robust to modest errors in the noise statistics.

**Index Terms**—Non-Gaussian noise, nonlinear detection, robustness, signal detection.

## I. INTRODUCTION

WHILE work in signal detection commonly assumes that the noise is Gaussian, there are important applications, such as lightning or ignition noise in radio frequencies, various impulsive noises in acoustics, where the noise is non-Gaussian or "heavy-tailed." As a result, the probability of encountering large magnitude noise values is much greater than predicted by Gaussian statistics. This departure from Gaussian statistics is especially important in the detection of weak signals.

This paper addresses binary-hypothesis testing for random signal detection in additive noise. For signal statistics known only to within a scaling factor, the signal-plus-noise case becomes a composite hypothesis, and one desires a uniformly most powerful (UMP) test that is optimum (in the Neyman-Pearson sense) for each possible signal scaling factor. Although UMP tests exist only in a few special cases when the noise is non-Gaussian [1], asymptotically optimum performance can be obtained for weak signals using a locally optimum (LO) test [1]. In general, the LO detector is a nonlinear processor. For a known signal or a white random signal in independent, identically distributed (i.i.d.) noise, the nonlinearity is memoryless, and the zero-memory nonlinearity (ZMNL) depends only on the marginal noise density. The LO test statistic for the known signal problem is a ZMNL (which is linear for Gaussian noise) followed by a correlator, and it has received much attention in the literature [1]. While fewer publications have addressed the random signal case, where the signal is an i.i.d. random process,

some earlier results on LO detection of random signals in additive i.i.d. noise [2], [3], [4] show that the LO test statistic is a ZMNL (which is linear for Gaussian noise), followed by an energy detector.

Much of the work on detecting deterministic signals, and virtually all of the reported work on detecting random signals, assumes complete and valid knowledge of the noise statistics. However, a recent paper [5] considers detection of weak random signals in generalized Gaussian noise with unknown variance. While other work on detection of deterministic signals shows that reasonably selected *ad hoc* nonlinearities provide nearly optimum performance over a range of noise densities [6], equivalent investigations of *ad hoc* nonlinearities and robustness have not been published for detectors of random signals.

## II. DETECTOR STRUCTURES

This section defines the detectors analyzed in this paper. Two circularly symmetric complex-valued non-Gaussian noise densities are introduced for use in numerical calculations and Monte Carlo simulations. The ZMNL for LO detectors and two *ad hoc* ZMNL's are defined in this section as well.

### A. Non-Gaussian Noise Densities

Throughout this paper, both signal and noise are assumed to be zero-mean complex-valued random processes, i.i.d. (the signal need only be white and wide-sense stationary)<sup>1</sup> and circularly symmetric [7]. The noise  $z$  has density  $f_z(z) = f_{z_R z_I}(z_R, z_I) = h(r)$ , where  $z$  has real and imaginary components  $z_R$  and  $z_I$  and modulus  $r = |z|$ , and  $f_r(r) = 2\pi r h(r)$ . One probability density function (pdf) for  $z$  used in the examples is the complex generalized Cauchy (GC) distribution [8], where  $z_R$  and  $z_I$  each have a GC distribution, with resulting pdf

$$f_{z_R}(x) = f_{z_I}(x) = \frac{\Gamma\left(\nu + \frac{1}{2}\right)}{\sqrt{\pi}\beta\Gamma(\nu)} \left[1 + \left(\frac{x}{\beta}\right)^2\right]^{-\nu - (1/2)}, \quad \nu > 0 \quad (2-1)$$

where  $\beta$  and  $\nu$  are scale parameters, and  $\Gamma(\cdot)$  is the gamma function. This is a special case of the GC distribution defined in [1] with  $k = 2$ . The GC pdf in (2-1) is equal to the Cauchy pdf when  $\nu = 1/2$  and approaches the Gaussian pdf as  $\nu \rightarrow \infty$ . The variance of the zero-mean complex random variable  $z$  is finite for

<sup>1</sup>It will be seen that the signal statistics only influence the detector structure and detection performance through the signal variance, which is assumed to exist.

Paper approved by S. G. Wilson, the Editor for Coding Theory and Applications of the IEEE Communications Society. Manuscript received March 17, 1997; revised August 28, 1998. This work was supported by the MITRE Sponsored Research Program.

The authors are with the MITRE Corporation, Bedford, MA 01730 USA.  
Publisher Item Identifier S 0090-6778(00)01581-6.

$\nu > 1$  and is given by  $\sigma_z^2 = E\{|z|^2\} = \beta^2/(\nu - 1)$ , with fourth moment  $E\{|z|^4\} = 2\beta^4/[(\nu - 1)(\nu - 2)]$ , which is finite for  $\nu > 2$ . The kurtosis parameter, defined as  $\kappa_z \triangleq E\{|z|^4\}/(2\sigma_z^4) - 1$ , is used to compare  $E\{|z|^4\}$  to the fourth moment of a complex Gaussian random variable with equal variance. From [8], the pdf of the modulus is

$$f_r(r) = \frac{2\nu r}{\beta^2} \left[ 1 + \left( \frac{r}{\beta} \right)^2 \right]^{-\nu-1}, \quad \nu > 0. \quad (2-2)$$

Another noise pdf used in the examples is the Gaussian–Gaussian mixture (GGM) distribution

$$f_z(z) = h(r) = \frac{1 - \varepsilon}{\pi\sigma_{\text{nom}}^2} e^{-(r^2/\sigma_{\text{nom}}^2)} + \frac{\varepsilon}{\pi\sigma_{\text{con}}^2} e^{-(r^2/\sigma_{\text{con}}^2)} \quad (2-3)$$

with mixture parameter  $0 \leq \varepsilon \leq 1$ , nominal variance  $\sigma_{\text{nom}}^2$ , and contamination variance  $\sigma_{\text{con}}^2$ . The variance and fourth moment of  $z$  are  $\sigma_z^2 = E\{|z|^2\} = (1 - \varepsilon)\sigma_{\text{nom}}^2 + \varepsilon\sigma_{\text{con}}^2$  and  $E\{|z|^4\} = (1 - \varepsilon)2\sigma_{\text{nom}}^4 + \varepsilon 2\sigma_{\text{con}}^4$ , respectively. The pdf of the modulus is

$$f_r(r) = 2r \left( \frac{1 - \varepsilon}{\sigma_{\text{nom}}^2} e^{-(r^2/\sigma_{\text{nom}}^2)} + \frac{\varepsilon}{\sigma_{\text{con}}^2} e^{-(r^2/\sigma_{\text{con}}^2)} \right). \quad (2-4)$$

### B. LO Detector

The complex-valued random observation vector  $X$  is  $X = \theta S + W$ , where  $\theta$  is the unknown, positive, real, weak-signal scaling factor, and  $S$  and  $W$  are random vectors corresponding to signal and noise, respectively;  $S$  is unit-variance, and  $W$  has variance  $\sigma_w^2$ . The detector tests the hypothesis  $\theta > 0$ . Under the assumptions above, the LO detector has test statistic  $t(X) = \sum_{j=1}^n g_{\text{LO}}^2(r_j)$ , where the LO nonlinearity is the memoryless transformation  $g_{\text{LO}}(r_j) = (\sigma_w^2/2)(\tilde{g}_{\text{LO}}(r_j) - \tilde{g}_{\text{LO}}(0))^{1/2}$ , with  $\tilde{g}_{\text{LO}}(r_j) = (h''(r_j)/h(r_j)) + (h'(r_j)/r_j h(r_j))$  [1], [2]. The LO test statistic is the energy in the observations at the output of the LO memoryless nonlinearity  $g_{\text{LO}}(\cdot)$ , and its form depends only on the pdf of the magnitude of the noise. For Gaussian noise, the LO nonlinearity  $g_{\text{LO}}(r) = r$ .

For the circularly symmetric GC pdf, the LO nonlinearity is

$$g_{\text{LO}}(r) = \frac{\beta r}{(\nu - 1)(\beta^2 + r^2)} \left( (\beta^2(\nu + 3) + r^2)(\nu + 1) \right)^{1/2} \quad (2-5)$$

or in terms of the noise variance  $\sigma_w^2$  and kurtosis parameter  $\kappa_w$

$$g_{\text{LO}}(r) = \frac{r\sigma_w}{(\kappa_w(r^2 + \sigma_w^2) + \sigma_w^2)} \left( \frac{(1 + 3\kappa_w)(\kappa_w(r^2 + 5\sigma_w^2) + \sigma_w^2(1 + 6\kappa_w))}{1 + \kappa_w} \right)^{1/2}. \quad (2-6)$$

Fig. 1 illustrates the LO nonlinearities for GC noise with unit variance for various values of the kurtosis parameter. For  $\kappa_w > 0$ , these LO nonlinearities limit the influence of large magnitude noise observations. In fact, for a fixed positive kurtosis parameter, the LO nonlinearity has the horizontal asymptote

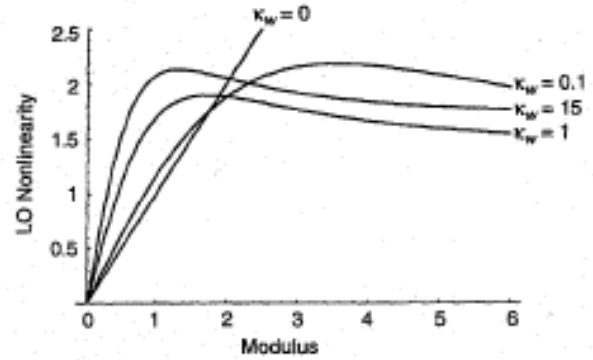


Fig. 1. LO nonlinearities for unit-variance GC noise with kurtosis parameter  $\kappa_w$ .

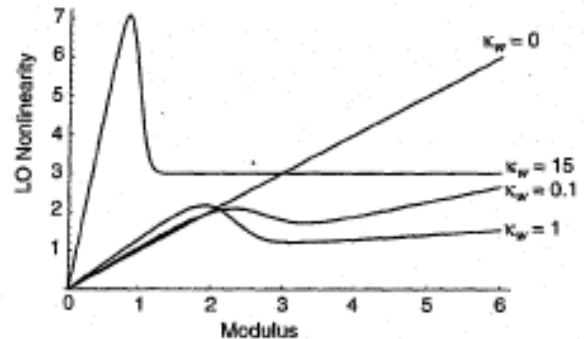


Fig. 2. LO nonlinearities for unit-variance GGM noise with kurtosis parameter  $\kappa_w$ .

$\lim_{r \rightarrow \infty} g_{\text{LO}}(r) = (\sigma_w^2(1 + 3\kappa_w)/(1 + \kappa_w))^{1/2}$ . In contrast, the LO detector for Gaussian noise has no nonlinearity to limit the effect of large modulus values from impulsive non-Gaussian noise.

For the circularly symmetric GGM pdf in (2-3), the LO nonlinearity is defined in (2-7), shown at the bottom of the next page. Fig. 2 illustrates the LO nonlinearities for GGM noise with unit variance, for various values of the kurtosis parameter. Since the GGM pdf is comprised of two Gaussian pdf's with different variances, the LO nonlinearities have two linear regions, one at small modulus values where the pdf with variance  $\sigma_{\text{nom}}^2$  dominates, and the other at large modulus values where the pdf with variance  $\sigma_{\text{con}}^2$  dominates. For finite  $\sigma_{\text{con}}^2$ , the LO nonlinearity is unbounded for large modulus values. Moreover, for large modulus values, there is no horizontal asymptote for GGM noise, indicating that its density has lighter tails than the GC density. If a GGM noise model is somewhat arbitrarily selected to provide robustness against non-Gaussian noise, the GGM LO detector may provide less robustness, since it implicitly assumes that far out in the tails, the noise exhibits Gaussian behavior, and these values need not be truncated as they are with the LO detector for GC noise.

### C. Ad Hoc Nonlinearities

The LO detector requires exact knowledge of the noise distribution. Since the noise distribution is usually not known, some simple detectors having a memoryless nonlinearity  $g(\cdot)$  that approximates the LO nonlinearity of interest. One such *ad hoc*

nonlinearity is the soft-limiter (SL) with breakpoint parameter  $a$ , defined as

$$g_{\text{SL}}(r) = \begin{cases} r, & 0 \leq r \leq a \\ a, & a \leq r. \end{cases} \quad (2-8)$$

The SL nonlinearity limits the influence of large-magnitude observations due to a heavy-tailed noise density by setting them equal to a constant.

The hole-puncher (HP) nonlinearity is identical to the SL nonlinearity for modulus values less than the breakpoint parameter, but it is equal to zero for inputs greater than  $a$

$$g_{\text{HP}}(r) = \begin{cases} r, & 0 \leq r \leq a \\ 0, & a < r. \end{cases} \quad (2-9)$$

### III. ASYMPTOTIC PERFORMANCE RESULTS

The performance of the LO detectors discussed in Section II depends on the signal amplitude parameter  $\theta$ , false alarm probability  $p_f$ , and the sample size  $n$ . Therefore, to determine the relative performance of a LO detector and some other detector, the detection probabilities must be computed for each triple  $(\theta, p_f, n)$  of interest. A more succinct way to compare two detectors is to compute their asymptotic relative efficiency (ARE) [1]. Under mild regularity conditions, the ARE is equal to the ratio of the efficacies of the two detectors.

#### A. Efficacy

The efficacy of a detector is defined in [1] and is related to deflection and output signal-to-noise ratio (SNR) under asymptotic conditions. For any detector whose form is that of the LO detector (ZMNL followed by an energy estimator), but with arbitrary ZMNL  $g(\cdot)$ , the efficacy is [9]

$$\eta(\psi, f_r) = \frac{1}{16} \frac{\left( \int_0^\infty \left[ \psi''(r) + \frac{\psi'(r)}{r} \right] f_r(r) dr \right)^2}{\int_0^\infty \psi^2(r) f_r(r) dr - \left( \int_0^\infty \psi(r) f_r(r) dr \right)^2} \quad (3-1)$$

where  $\psi(\cdot) = g^2(\cdot)$ .

This result is a very general expression for describing detection performance. It yields the efficacy for any ZMNL (or no nonlinearity at all) and any circularly symmetric noise density (including Gaussian noise). Since the test statistic is Gaussian-distributed under these asymptotic conditions, efficacy is also directly related to the operating characteristic (detection probability, false alarm probability). Consequently,

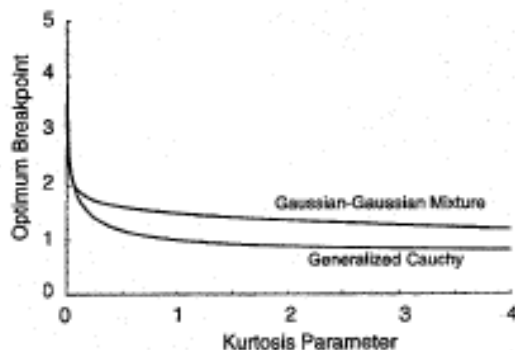


Fig. 3. SL breakpoint parameter that optimizes efficacy.

(3-1) can be used to predict performance of LO and sub-optimum detectors over a range of conditions, without the limitations and demands of Monte Carlo simulations.

Expressions for efficacies of detectors under consideration are given in the appendix. Numerical optimization of (A-2) and (A-3) yields the breakpoint parameters that maximize the SL's efficacy for specific noise density parameters. Fig. 3 shows the optimum SL breakpoint parameter for the GC and GGM noise models with unit variance and specific kurtosis parameters. For very small kurtosis parameters, the optimum breakpoint parameter is very large, showing that the detector approaches the square-law (SQ) detector that is optimum for Gaussian noise. As the kurtosis parameter becomes large, the optimum breakpoint parameter appears to approach asymptotic values near the standard deviation of the noise, with the horizontal asymptote for the GGM noise somewhat larger than that for the GC noise.

Numerical optimization of (A-5) and (A-6) yields breakpoint parameters that maximize the efficacy of the HP for specific noise density parameters. The optimum breakpoint parameter for the GGM and GC noise densities with unit variance and specific kurtosis parameters [9] is similar qualitatively to those in Fig. 3. For very small kurtosis parameters, the optimum breakpoint parameter is very large, i.e., the detector approaches the SQ detector that is optimum for Gaussian noise. As the kurtosis parameter becomes large, the optimum breakpoint parameters appear to approach asymptotic values near twice the standard deviation of the noise, with almost equal horizontal asymptotes for the GGM noise and the GC noise.

Interestingly, the efficacy of the SQ detector, (A-7), depends only on the kurtosis parameter, and not on moments of higher order than four. This is similar to the known signal problem, where the efficacy of the linear correlator depends only on the variance of the noise and not on moments of order higher than two.

$$g_{\text{LO}}(r) =$$

$$\frac{((1-\varepsilon)\sigma_{\text{nom}}^2 + \varepsilon\sigma_{\text{con}}^2)}{\sigma_{\text{nom}}\sigma_{\text{con}}} \left( \frac{(1-\varepsilon)\sigma_{\text{con}}^4 + \varepsilon\sigma_{\text{nom}}^4}{((1-\varepsilon)\sigma_{\text{con}}^2 + \varepsilon\sigma_{\text{nom}}^2)} + \frac{(1-\varepsilon)(r^2 - \sigma_{\text{nom}}^2)\sigma_{\text{con}}^6 e^{(r^2/\sigma_{\text{con}}^2)} + \varepsilon(r^2 - \sigma_{\text{con}}^2)\sigma_{\text{nom}}^6 e^{(r^2/\sigma_{\text{nom}}^2)}}{\sigma_{\text{nom}}^2\sigma_{\text{con}}^2((1-\varepsilon)\sigma_{\text{con}}^2 e^{(r^2/\sigma_{\text{con}}^2)} + \varepsilon\sigma_{\text{nom}}^2 e^{(r^2/\sigma_{\text{nom}}^2)})} \right)^{1/2} \quad (2-7)$$

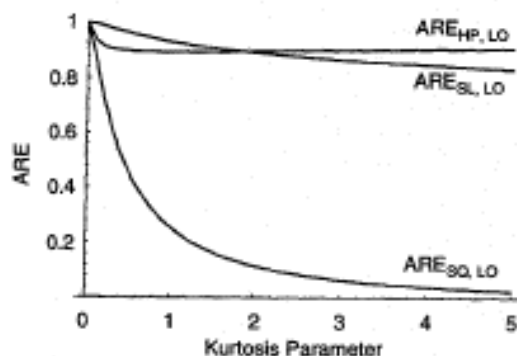


Fig. 4. ARE for SL, HP, and SQ detectors relative to the LO detector for GGM noise.

### B. ARE

Assuming some mild regularity conditions, it can be shown [1] that the ARE of a detector  $A$  with respect to a detector  $B$  is given by the ratio of their efficacies. Fig. 4 shows the ARE for GGM noise of the SL, HP, and SQ detectors with respect to the LO detector as a function of the kurtosis parameter. The breakpoint parameters of the SL and HP detectors are chosen to maximize their efficacies at each value of kurtosis parameter. Therefore,  $ARE_{SL,LO}$  and  $ARE_{HP,LO}$  in Fig. 4 are the ARE's of the optimum SL and HP detectors relative to the LO detector.

When the kurtosis parameter is zero, the noise is Gaussian and the SQ detector is LO. Hence,  $ARE_{SQ,LO} = ARE_{SQ,SQ} = 1$ . The optimum breakpoint parameters of the SL and HP detectors are theoretically infinite for Gaussian noise, and the SL and HP detectors are equivalent to the SQ detector. Therefore,  $ARE_{SL,LO} = ARE_{HP,LO} = 1$  at a kurtosis parameter of zero.

The crossing of the  $ARE_{SL,LO}$  and  $ARE_{HP,LO}$  curves in Fig. 4 can be explained by considering the similarities of the SL, HP, and LO nonlinearities in Fig. 2 for small and large kurtosis parameters. For small values of kurtosis parameter, the LO nonlinearity is similar to the SL nonlinearity. Both have a linear region for smaller magnitudes and approximate a constant for larger magnitudes. For large values of kurtosis parameter, the LO nonlinearity more closely resembles the HP nonlinearity, with a linear region for small magnitudes and then an almost discontinuous drop to a smaller output like the HP nonlinearity.

The predicted poor performance of the SQ detector from  $ARE_{SQ,LO}$  for larger kurtosis parameter values can also be explained by comparing nonlinearities. The larger the kurtosis parameter value, the higher the probability of large noise magnitudes. The SQ detector does nothing to mitigate the effects of these large noise magnitudes the way the SL, HP, and LO detectors do, and it allows these large values to contaminate the test statistic.

Calculation of the ARE for GC noise of the SL, HP, and SQ detectors with respect to the LO detector as a function of the kurtosis parameter, using the breakpoint parameters chosen to maximize the performance of the SL and HP detectors relative to the LO detector, produces results qualitatively similar to Fig. 4. These results can be explained by comparing the LO nonlinearity for GC noise in Fig. 1 to the SL and HP nonlinearities. The SL detector performs essentially as well as the LO detector

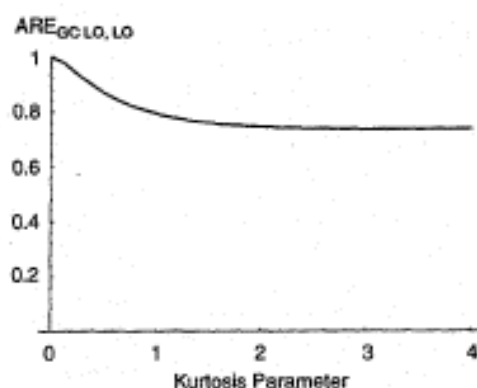


Fig. 5. ARE of LO detector assuming GC noise when actual noise is GGM.

over the kurtosis parameter range shown. This is not surprising considering the similarity of the SL and LO nonlinearities in this kurtosis parameter range. The performance of the HP detector is predicted to be worse in GC noise than it is in GGM noise. This is because the LO nonlinearity does not have the shape of the HP nonlinearity for larger kurtosis parameter values like the LO nonlinearity for GGM noise.

Other results [9] predict poor performance for the SQ detector in GC noise, similar to the performance in GGM noise.

### C. Robustness

Two different types of robustness are evaluated. In the first type, the kurtosis parameter is correct, but the noise arises from a different distribution than that assumed. In the second type, the noise distribution parametric form is correct, but the assumed kurtosis parameter differs from the actual kurtosis parameter of the noise.

Fig. 5 shows the robustness of the LO detector when the true kurtosis parameter is known, but the wrong noise distribution is assumed. The LO reference detector in the ARE assumes the correct noise distribution. The ARE results in Fig. 5 are for an LO detector designed for GC noise when the actual noise is GGM. Over the kurtosis parameter range shown, similar results are obtained when the LO detector is designed for GGM noise when the actual noise is GC. As the kurtosis parameter tends to zero, the ARE = 1 since the noise models approach Gaussian. The behavior can be explained by considering the LO nonlinearities in Figs. 1 and 2. As the kurtosis parameter begins to increase from zero, the ARE rapidly degrades because the LO nonlinearities of the two noise models begin to take different shapes. In particular, for a kurtosis parameter equal to one, the slope of the GC LO nonlinearity at the origin is about twice that of the GGM LO nonlinearity. For these smaller values of kurtosis parameter, the tail of the noise density is relatively light, and the noise values with magnitudes close to the origin have a large effect on performance. For larger values of kurtosis parameter, the tail of the noise density has more of an effect on performance, and the ARE is relatively constant. This relatively constant ARE for larger kurtosis parameter values can be explained by looking at the LO nonlinearities for large magnitudes. Both nonlinearities limit the output magnitude to a relatively constant value.

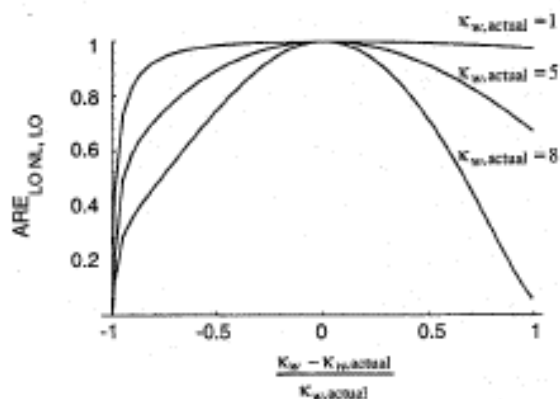


Fig. 6. ARE of LO detector assuming kurtosis parameter  $\kappa_w$  relative to LO detector with true kurtosis parameter  $\kappa_{w,actual}$  for GGM noise.

Consequently, if the noise kurtosis is known, but the density is wrong (at least between the two densities considered here), there is little degradation of LO detector performance.

Fig. 6 shows the sensitivity of the LO detector to deviations in the actual noise kurtosis parameter  $\kappa_w$  for GGM noise. The figure shows the ARE of a detector using the LO nonlinearity derived using the correct noise density parametric form but an incorrect  $\kappa_w$ , relative to the LO detector with the correct noise density parametric form and the correct  $\kappa_w$ , as a function of the relative kurtosis error. For a reasonable estimate of  $\kappa_{w,actual}$ , the relative error is near zero and the detector performs well. The reason that an LO detector designed for GC noise is more robust for large deviations from  $\kappa_{w,actual}$  can again be seen from the LO nonlinearities in Fig. 2. The shape of the LO nonlinearity for GGM noise varies tremendously over the kurtosis values shown, but the LO nonlinearities for GC noise retain similar shape. Analogous results for GC noise have different character; the curves maintain a value near unity for all positive values on the abscissa.

When the noise is GGM, the curves are approximately symmetric, showing that the effect of either underestimating or overestimating the kurtosis parameter is similar. For GC noise, however, it is far better to overestimate the kurtosis parameter and use an LO detector designed for a larger kurtosis parameter than may be actually encountered.

Fig. 6 also shows the well-known poor performance when a detector designed for Gaussian noise is used in impulsive non-Gaussian noise. At a relative error of  $-1$ ,  $\kappa_w = 0$  and  $ARE_{LO,NL,LO} = ARE_{SQ,LO}$ .

For the SL detector and the HP detector, robustness involves evaluating the effect of suboptimum breakpoint parameters. Figs. 7 and 8 show the sensitivity of these *ad hoc* detectors to deviations from the optimum breakpoint parameter  $a_0$  that maximizes their efficacy. The figures plot the ARE of the *ad hoc* detector for GGM noise, using breakpoint  $a$ , with respect to the *ad hoc* detector using the optimum breakpoint parameter for each value of kurtosis parameter, as a function of the relative error. Qualitatively similar results are obtained [9] for GC noise.

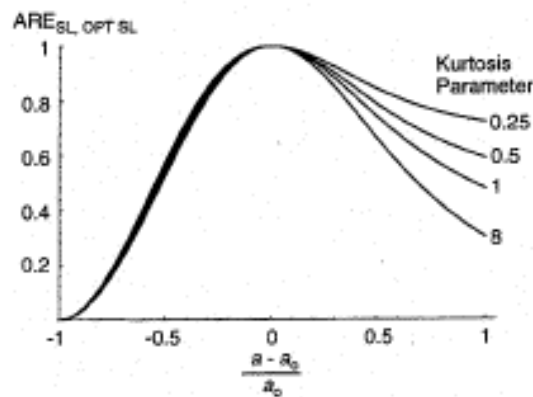


Fig. 7. ARE of SL detector with breakpoint parameter  $a$  relative to optimum SL (OPT SL) detector with optimum breakpoint parameter  $a_0$  for GGM noise.

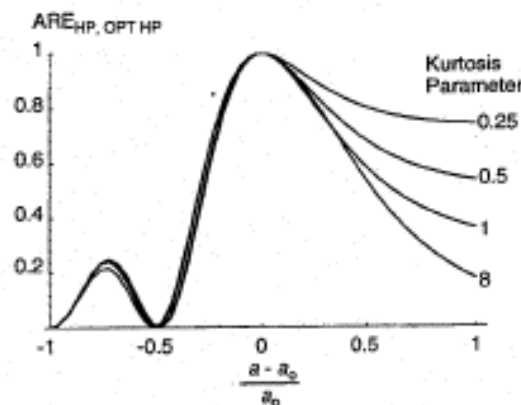


Fig. 8. ARE of HP detector with breakpoint parameter  $a$  relative to optimum HP (OPT HP) detector with optimum breakpoint parameter  $a_0$  for GGM noise.

The shape of the curves in all of these figures is broad about zero relative error, indicating robustness with respect to breakpoint parameter, whether the error is caused by incorrect estimation of the kurtosis parameter or of the noise density, or both. For these two noise distribution parametric forms, the shape of the SL is broader about zero relative error than the HP, and it is therefore more robust with respect to the breakpoint parameter. Moreover, it is better to err on the side of making the breakpoint parameter too large, rather than making it too small, which degrades performance more severely.

#### D. Operating Characteristics

When the sample size of the LO detector is large enough for the test statistic to have a Gaussian distribution by the central limit theorem, and the signal is sufficiently weak for the variance of the test statistic to be the same under both hypotheses, the results from asymptotic analysis can be readily translated to operating characteristics. Under these assumptions, it can be shown that the detection probability  $p_d$  as a function of the output SNR  $\rho_o$  and false-alarm probability  $p_f$  is

$$p_d = \Phi(\sqrt{\rho_o} + \Phi^{-1}(p_f)) \quad (3-2)$$

where  $\Phi(\cdot)$  is the standard Gaussian cumulative distribution function and  $\rho_o$ , the output SNR (identical to the squared deflection), is defined as

$$\rho_o = \frac{(\mathbb{E}\{t(X) | H_1\} - \mathbb{E}\{t(X) | H_0\})^2}{\text{Var}\{t(X) | H_0\}}. \quad (3-3)$$

Since the test statistics of interest have the form  $t(X) = \sum_{j=1}^n \psi(|x_j|)$ , then for sufficiently large  $n$ ,  $\rho_o \cong \eta(\psi, f_r) n \rho_i^2$ , where  $\eta(\psi, f_r)$  is the efficacy for nonlinearity  $\psi(\cdot)$  and noise density  $f_r(\cdot)$ , and  $\rho_i = \theta^2$  is the input SNR, since the noise variance is unity. Therefore, for a fixed large  $n$ , a given  $p_f$ , and small  $\rho_i$ , the detection probability can be approximated from (3-2) by computing the efficacy  $\eta(\psi, f_r)$  and using

$$p_d = \Phi(\rho_i \sqrt{\eta(\psi, f_r) n} + \Phi^{-1}(p_f)). \quad (3-4)$$

#### IV. MONTE CARLO SIMULATIONS

The ratio of the number of samples that two detectors need to obtain the same detection performance is defined as the relative efficiency (RE). Under mild regularity conditions, the RE approaches the ARE as the sample size gets large [1]. Since any practical detection problem has a finite sample size, the RE is a more accurate relative performance measure than ARE. However, the ARE is more readily determined analytically; determining the RE usually requires extensive Monte Carlo simulations.

Previously reported simulation results [1], [10], [11] for deterministic signals indicate that very large sample sizes are required for the RE to approach the ARE for some detectors and noise distributions. This section compares the RE from Monte Carlo simulations to the ARE results presented in Section III for a random signal in GC and GGM noise, indicating the sample size required before analytical results derived under asymptotic assumptions can be applied.

The simulations use samples of a white, stationary, circularly symmetric Gaussian signal added to i.i.d. circularly symmetric noise. The unit-variance noise distribution is from either the GC family or the GGM family. Since the noise distributions are parameterized by the kurtosis parameter, each kurtosis parameter of interest requires a set of Monte Carlo trials, run for kurtosis parameter increments of 0.1. The GC noise has one free parameter to determine the kurtosis parameter. Since GGM noise has two free parameters, the contamination parameter  $\epsilon$  is set equal to 0.05, so that samples from the contamination distribution occur, on the average, five times within 100 samples, ensuring that almost all realizations of a hundred samples or more include samples from the contamination distribution.

Simulations were run to determine the number of samples required by a detector to provide the desired operating point  $p_d = 0.5$  and  $p_f = 0.01$  at an input SNR of  $\rho_i = -10$  dB. The detectors used in the simulations are the same ones used in the analytical results of Section III: the LO, SQ, SL, and HP detectors. Results are for  $10^4$  and  $10^5$  independent Monte Carlo trials.

An iterative approach is used to determine the sample size needed to obtain the desired operating point. For the selected

TABLE I

NUMBER OF SAMPLES REQUIRED TO OBTAIN OPERATING POINT  $p_d = 0.5$  AND  $p_f = 0.01$  AT INPUT SNR OF  $-10$  dB FOR GGM AND GC NOISE

Detector	Noise Model	Required Number of Samples	
		Noise Kurtosis = 0	Noise Kurtosis = 4
Square Law (SQ)	GGM	578	5255
	GC	571	6263
Soft Limiter (SL)	GGM	571	300
	GC	581	494
Hole Puncher (HP)	GGM	571	270
	GC	581	759

operating point, use the asymptotic result in (3-4) to obtain an initial estimate of the required sample size. Synthesize noise-only realizations and signal-plus-noise realizations at the stated input SNR, and generate test statistics for each realization and each hypothesis. Use the noise-only test statistics to obtain the threshold setting that provides the desired fraction of false alarms, then determine the fraction of detections using this threshold for the signal-plus-noise test statistics. In our experience, the result is less than the desired detection probability. Increase the sample size by moderate amounts until the measured fraction of detections exceeds the desired detection probability, then interpolate to estimate the sample size needed for the desired detection probability.

The results, summarized in Table I, show that the SQ detector is not robust to heavy-tailed noise, requiring many more samples (i.e., a longer integration time) to obtain the same operating point in GGM and GC noise. In contrast, nonlinear detectors that are reasonably matched to the non-Gaussian noise density provide better performance (i.e., shorter integration times to obtain the same operating point) in non-Gaussian noise than any detector obtains in Gaussian noise with the same variance.

Figs. 9 and 10 compare the RE and ARE of the *ad hoc* detectors relative to the LO detector for GGM noise; additional, similar results are provided in [9]. The smooth curve is the analytically calculated ARE, and the more jagged curve is the RE for  $10^4$  independent trials. Data points denoted by X's at integer values of kurtosis parameter are results for  $10^5$  independent trials; these points should have less variance than the RE curve for  $10^4$  independent trials.

For the SQ detector in GGM noise, the RE curve is relatively smooth because of the large sample size required by the SQ detector to obtain the desired performance in impulsive non-Gaussian noise. Results for the SL detector in GGM noise are shown in Fig. 9. Since the SL detector outperforms the SQ detector in non-Gaussian noise, smaller sample sizes are required for the same performance. However, the smaller sample size creates higher statistical variance in the RE data. The RE data follow the ARE quite well for small kurtosis parameter values, but the RE falls slightly below the ARE for the larger kurtosis parameter values. Fig. 10 shows that the ARE accurately predicts the finite sample size performance of RE for the given input SNR, operating point, and GGM noise

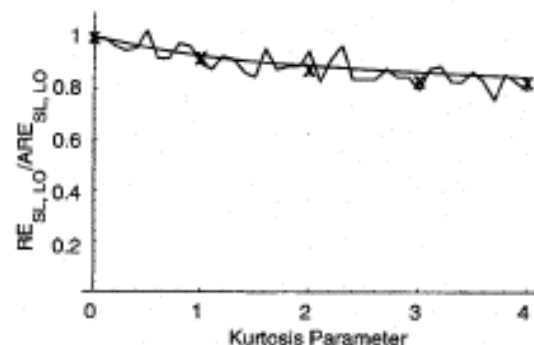


Fig. 9. RE and ARE of SL detector relative to LO detector for GGM noise.

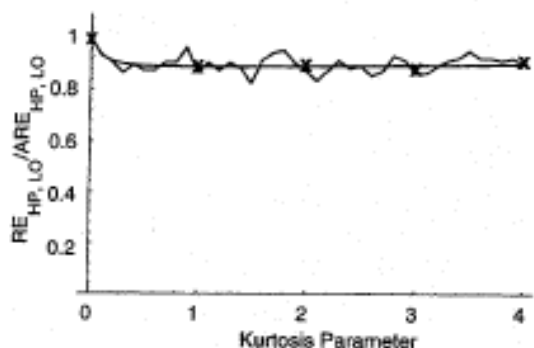


Fig. 10. RE and ARE of HP detector relative to LO detector for GGM noise.

over the kurtosis parameter range shown. However, results in [9] show that the ARE of the HP detector gives a slightly inaccurate prediction for GC noise.

While these results apply only for the specific detection probability, false alarm probability, and noise densities that were considered, the following generalizations are suggested.

- For the cases considered, the asymptotic results are very accurate—typically the asymptotic (theoretically predicted) observation size is within 10% of the size measured using Monte Carlo simulations. Since the simulations require considerable computational resources, using the asymptotic results is preferred and appears to be justified.
- As the detection performance improves (higher detection probabilities, lower false alarm probabilities), more samples would be required, and consequently one would expect the asymptotic results to be even more accurate.
- Simulating the SQ detector in heavy-tailed noise is particularly computationally demanding for several reasons. Since the SQ detector has low efficacy, a large number of samples must be used to achieve the requisite detection performance. Also, since large-magnitude samples are not attenuated, they produce large-variance contributions to the test statistic, requiring more samples for the test statistic to approach a Gaussian distribution. While working at a higher input SNR can avert the first problem,

it does not help solve the second problem and may violate the weak signal assumption inherent to this processing and analysis.

- There appears to be little significant distinction between the experimental and asymptotic results obtained with the two *ad hoc* nonlinearities and the two noise densities.

## V. SUMMARY

Qualitatively, the behavior of LO detectors and detectors using *ad hoc* ZMNL's for random signals in non-Gaussian noise closely corresponds to behavior previously reported for known signals in non-Gaussian noise. The performance of the SQ detector, which is the LO detector for Gaussian noise, degrades substantially as the noise becomes heavier tailed than Gaussian. Better performance can be obtained with optimum processing in non-Gaussian noise than with optimum processing in Gaussian noise, for the same input SNR and observation time. The *ad hoc* SL and HP detectors have nonlinearities that approximate LO nonlinearities and thus are effective in restoring and even enhancing the performance lost by the SQ detector in non-Gaussian noise. Each of these *ad hoc* detectors has a nonlinearity consisting of two piecewise-linear regions separated by a breakpoint parameter. The *ad hoc* detectors can be used without knowledge of the noise distribution, but if the noise distribution is known, their breakpoint parameter can be chosen to optimize performance. When the *ad hoc* detectors use the optimum breakpoint parameter, they provide near-optimum performance in the noise densities considered. At least for the classes of non-Gaussian noise considered, the SL nonlinearity is generally preferred to the HP.

Expressions are provided to calculate the asymptotic performance of a broad class of detectors (including optimum and sub-optimum nonlinearities) in any noise distribution. Expressions were also used to predict detector performance and to evaluate detector robustness to errors in the noise models, using several different types of modeling errors. The results indicate that using an LO detector, even assuming an incorrect noise distribution, is much better than using the SQ detector in non-Gaussian noise. The results also show that the *ad hoc* detectors are robust with respect to their breakpoint parameter.

Since the analytical performance results are asymptotic as the observation time goes to infinity and the signal power goes to zero, Monte Carlo simulations involving finite observation times and nonzero signal power were used to ascertain the applicability of the asymptotic results. The conclusion of this evaluation is that the asymptotic results are very accurate for the conditions examined.

## APPENDIX EFFICACY EXPRESSIONS

Using (3-1), the efficacy of a detector with the SL nonlinearity in (2-8) is defined in (A-1), shown at the bottom of the next page. For a given  $f_r(\cdot)$ , an optimum  $a$  can be chosen to maximize  $\eta(\psi_{SL}, f_r)$ .

Substituting (2-2) into (A-1) and expressing the noise density parameters in terms of the noise kurtosis parameter  $\kappa_w$  yields the efficacy of the SL detector for unit-variance GC noise

$$\begin{aligned} \eta(\psi_{\text{SL}}, \text{GC}) &= \left( 1 - \frac{1}{\left(1 + \frac{a^2 \kappa_w}{\kappa_w + 1}\right)^{2+(1/\kappa_w)}} \right. \\ &\quad \left. - \frac{(\kappa_w + 1)^2 (2\kappa_w + 1) a^2}{(a^2 \kappa_w + \kappa_w + 1)^3 \left(1 + \frac{a^2 \kappa_w}{\kappa_w + 1}\right)^{(1/\kappa_w)}} \right)^2 \\ &\quad \cdot \left[ 2(\kappa_w + 1) - \frac{2(a^4 \kappa_w + a^2(2\kappa_w + 1) + \kappa_w + 1)}{\left(1 + \frac{a^2 \kappa_w}{\kappa_w + 1}\right)^{2+(1/\kappa_w)}} \right. \\ &\quad \left. - \left( 1 - \frac{a^2 \kappa_w + \kappa_w + 1}{(\kappa_w + 1) \left(1 + \frac{a^2 \kappa_w}{\kappa_w + 1}\right)^{2+(1/\kappa_w)}} \right)^2 \right]^{-1}. \end{aligned} \quad (\text{A-2})$$

Substituting (2-4) into (A-1) and expressing the noise density parameters in terms of the noise kurtosis parameter  $\kappa_w$  yields the efficacy of the SL detector for unit-variance GGM noise

$$\begin{aligned} \eta(\psi_{\text{SL}}, \text{GGM}) &= \left( 1 - (1 - \varepsilon) \left( 1 + \frac{a^2}{\sigma_{\text{nom}}^2} \right) e^{-(a^2/\sigma_{\text{nom}}^2)} \right. \\ &\quad \left. - \varepsilon \left( 1 + \frac{a^2}{\sigma_{\text{con}}^2} \right) e^{-(a^2/\sigma_{\text{con}}^2)} \right)^2 \\ &\quad \cdot \left[ 2(1 - \varepsilon) \sigma_{\text{nom}}^2 \left( \sigma_{\text{nom}}^2 - (a^2 + \sigma_{\text{nom}}^2) e^{-(a^2/\sigma_{\text{nom}}^2)} \right) \right. \\ &\quad \left. + 2\varepsilon \sigma_{\text{con}}^2 \left( \sigma_{\text{con}}^2 - (a^2 + \sigma_{\text{con}}^2) e^{-(a^2/\sigma_{\text{con}}^2)} \right) \right. \\ &\quad \left. - \left\{ 1 + (1 - \varepsilon) \left( \sigma_{\text{nom}}^2 \left( 1 - e^{-(a^2/\sigma_{\text{nom}}^2)} \right) - 1 \right) \right. \right. \\ &\quad \left. \left. + \varepsilon \left( \sigma_{\text{con}}^2 \left( 1 - e^{-(a^2/\sigma_{\text{con}}^2)} \right) - 1 \right) \right\}^2 \right]^{-1}. \end{aligned} \quad (\text{A-3})$$

where  $\sigma_{\text{nom}}^2 = 1 - \sqrt{\varepsilon \kappa_w / (1 - \varepsilon)}$  and  $1 + \sqrt{((1 - \varepsilon) \kappa_w / \varepsilon)}$ .

Similarly, substituting (2-9) into (3-1) yields the efficacy of the HP detector

$$\eta(\psi_{\text{HP}}, f_r) = \frac{1}{16} \frac{\left( 4 \int_0^a f_r(r) dr - 3a f_r(a) + a^2 f_r'(a) \right)^2}{\int_0^a r^4 f_r(r) dr - \left( \int_0^a r^2 f_r(r) dr \right)^2}. \quad (\text{A-4})$$

For a given  $f_r(\cdot)$ , an optimum  $a$  can be chosen to maximize  $\eta(\psi_{\text{HP}}, f_r)$ .

The efficacy of the HP detector for unit-variance GC noise as a function of noise kurtosis parameter  $\kappa_w$  is

$$\begin{aligned} \eta(\psi_{\text{HP}}, \text{GC}) &= \left( 1 - \frac{1}{\left(1 + \frac{a^2 \kappa_w}{\kappa_w + 1}\right)^{2+(1/\kappa_w)}} \right. \\ &\quad \left. - \frac{(\kappa_w + 1)^2 (2\kappa_w + 1) ((4\kappa_w + 1)a^4 + a^2 \kappa_w + a^2)}{(a^2 \kappa_w + \kappa_w + 1)^3 \left(1 + \frac{a^2 \kappa_w}{\kappa_w + 1}\right)^{(1/\kappa_w)}} \right)^2 \\ &\quad \cdot \left[ 2(\kappa_w + 1) - \frac{(2\kappa + 1)(a^4 + 2a^2 + 1) + 1}{\left(1 + \frac{a^2 \kappa_w}{\kappa_w + 1}\right)^{2+(1/\kappa_w)}} \right. \\ &\quad \left. - \left( 1 - \frac{(2\kappa_w + 1)a^2 + \kappa_w + 1}{(\kappa_w + 1) \left(1 + \frac{a^2 \kappa_w}{\kappa_w + 1}\right)^{2+(1/\kappa_w)}} \right)^2 \right]^{-1}. \end{aligned} \quad (\text{A-5})$$

The efficacy of the HP detector for unit-variance GGM noise is

$$\begin{aligned} \eta(\psi_{\text{HP}}, \text{GGM}) &= \left( 1 - (1 - \varepsilon) \left( 1 + \frac{a^2}{\sigma_{\text{nom}}^2} + \frac{a^4}{\sigma_{\text{nom}}^4} \right) e^{-(a^2/\sigma_{\text{nom}}^2)} \right. \\ &\quad \left. - \varepsilon \left( 1 + \frac{a^2}{\sigma_{\text{con}}^2} + \frac{a^4}{\sigma_{\text{con}}^4} \right) e^{-(a^2/\sigma_{\text{con}}^2)} \right)^2 \left[ (1 - \varepsilon) \right. \\ &\quad \cdot \left( 2\sigma_{\text{nom}}^4 - (a^4 + 2\sigma_{\text{nom}}^2(a^2 + \sigma_{\text{nom}}^2)) e^{-(a^2/\sigma_{\text{nom}}^2)} \right) \\ &\quad \left. + \varepsilon \left( 2\sigma_{\text{con}}^4 - (a^4 + 2\sigma_{\text{con}}^2(a^2 + \sigma_{\text{con}}^2)) e^{-(a^2/\sigma_{\text{con}}^2)} \right) \right. \\ &\quad \left. - \left\{ (1 - \varepsilon) \left( \sigma_{\text{nom}}^2 - (a^2 + \sigma_{\text{nom}}^2) e^{-(a^2/\sigma_{\text{nom}}^2)} \right) \right. \right. \\ &\quad \left. \left. + \varepsilon \left( \sigma_{\text{con}}^2 - (a^2 + \sigma_{\text{con}}^2) e^{-(a^2/\sigma_{\text{con}}^2)} \right) \right\}^2 \right]^{-1}. \end{aligned} \quad (\text{A-6})$$

The efficacy of the SQ detector is equal to the efficacy of the SL and HP detectors when  $a \rightarrow \infty$  and is given by

$$\eta(\psi_{\text{SQ}}) = \frac{1}{2\kappa_w + 1}. \quad (\text{A-7})$$

It can be shown [9] that the LO nonlinearity maximizes the efficacy (3-1), which is

$$\eta(\psi_{\text{LO}}, f_r) = \frac{1}{16} \int_0^\infty \left[ \frac{h''(r)}{h(r)} + \frac{h'(r)}{r h(r)} \right]^2 f_r(r) dr. \quad (\text{A-8})$$

#### ACKNOWLEDGMENT

The authors thank the reviewers for perceptive suggestions that improved this paper.

$$\eta(\psi_{\text{SL}}, f_r) = \frac{1}{16} \frac{\left( 4 \int_0^a f_r(r) dr - 2a f_r(a) \right)^2}{\int_0^a r^4 f_r(r) dr + a^4 \int_a^\infty f_r(r) dr - \left( \int_0^a r^2 f_r(r) dr + a^2 \int_a^\infty f_r(r) dr \right)^2}. \quad (\text{A-1})$$

## REFERENCES

- [1] S. A. Kassam, *Signal Detection in Non-Gaussian Noise*. New York: Springer-Verlag, 1988.
- [2] H. V. Poor and J. B. Thomas, "Locally optimum detection of discrete-time stochastic signals in non-Gaussian noise," *J. Acoust. Soc. Amer.*, vol. 63, pp. 75-80, Jan. 1978.
- [3] J. J. Sheehy, "Optimum detection of signals in non-Gaussian noise," *J. Acoust. Soc. Amer.*, vol. 63, pp. 81-90, Jan. 1978.
- [4] N. H. Lu and B. A. Eisenstein, "Detection of weak signals in non-Gaussian noise," *IEEE Trans. Inform. Theory*, vol. IT-27, pp. 755-771, Nov. 1981.
- [5] L. Izzo, L. Paura, and M. Tanda, "Signal interception in non-Gaussian noise," *IEEE Trans. Commun.*, vol. 40, pp. 1030-1037, June 1992.
- [6] J. H. Miller and J. B. Thomas, "Robust detectors for signals in non-Gaussian noise," *IEEE Trans. Commun.*, vol. COM-25, pp. 686-690, July 1977.
- [7] F. D. Neeser and J. L. Massey, "Proper complex random processes with applications to information theory," *IEEE Trans. Inform. Theory*, vol. 39, pp. 1293-1302, July 1993.
- [8] J. W. Modestino and A. Y. Ningo, "Detection of weak signals in narrow-band non-Gaussian noise," *IEEE Trans. Inform. Theory*, vol. IT-25, pp. 592-600, Sept. 1979.
- [9] K. R. Kolodziejcki and J. W. Betz, "Detection of Weak Random Signals in Stationary Non-Gaussian Noise," The MITRE Corporation, Bedford, MA, Tech. Rep. MTR95B53, Apr. 1995.
- [10] D. L. Michalsky, G. L. Wise, and H. V. Poor, "A relative efficiency study of some popular detectors," *J. Franklin Inst.*, vol. 313, pp. 135-148, Mar. 1982.
- [11] M. I. Dadi and R. J. Marks II, "Detector relative efficiencies in the presence of Laplace noise," *IEEE Trans. Aerosp. Electron. Syst.*, vol. AES-23, pp. 568-582, July 1987.